On the Mechanism of the Reaction Catalyzed by Glucose 6-Phosphate Dehydrogenase † , ‡

ARTICLE *in* BIOCHEMISTRY · APRIL 1998

Impact Factor: 3.02 · DOI: 10.1021/bi972069y · Source: PubMed

5 AUTHORS, INCLUDING:

Claire E Naylor
Birkbeck, University of London
55 PUBLICATIONS **1,402** CITATIONS
SEE PROFILE

Margaret Adams
University of Oxford
62 PUBLICATIONS **2,046** CITATIONS
SEE PROFILE

On the Mechanism of the Reaction Catalyzed by Glucose 6-Phosphate Dehydrogenase[†,‡]

Michael S. Cosgrove,[§] Claire Naylor,[||] Søren Paludan,[||] Margaret J. Adams,[||] and H. Richard Levy*[,§]

Department of Biology, Syracuse University, Syracuse, New York 13244, and Laboratory of Molecular Biophysics, University of Oxford, Oxford OX1 3QU, United Kingdom

Received August 20, 1997; Revised Manuscript Received November 17, 1997

ABSTRACT: The catalytic mechanism of glucose 6-phosphate dehydrogenase from *Leuconostoc mesenteroides* was investigated by replacing three amino acids, His-240, Asp-177, and His 178, with asparagine, using site-directed mutagenesis. Each of the mutant enzymes was purified to homogeneity and characterized by substrate binding studies and steady-state kinetic analyses. The three-dimensional structure of the H240N glucose 6-phosphate dehydrogenase was determined at 2.5 Å resolution. The results support a mechanism in which His-240 acts as the general base that abstracts the proton from the C1-hydroxyl group of glucose 6-phosphate, and the carboxylate group of Asp-177 stabilizes the positive charge that forms on His-240 in the transition state. The results also confirm the postulated role of His-178 in binding the phosphate moiety of glucose 6-phosphate.

Glucose 6-phosphate dehydrogenase (G6PD, EC 1.1.1.49)[1] catalyzes the oxidation of glucose 6-phosphate (G6P) using $NADP^+$ and/or NAD^+. In mammals, this enzyme uses $NADP^+$ to catalyze the first committed step of the pentose phosphate pathway which yields reducing equivalents in the form of NADPH for reductive biosynthesis and protection from oxidative stress, and five-carbon sugars for the synthesis of nucleotides. The G6PD from the microorganism *Leuconostoc mesenteroides* has been studied in great detail due to its unusual dual-coenzyme specificity (reviewed in ref *1*). When $NADP^+$ is the coenzyme, the kinetic mechanism of this enzyme is ordered sequential with $NADP^+$ binding first; when NAD^+ is the coenzyme, the kinetic mechanism is steady-state random (*2*). Evidence has been presented that the binding of $NADP^+$ and of NAD^+ engender different conformations of the enzyme (*3*). The enzyme from *L. mesenteroides* has been cloned and expressed in *Escherichia coli* (*4*), and the structure of the apo-enzyme, crystallized from 3.0 M phosphate, has been solved to a resolution of 2.0 Å (*5*). This has led to the identification of an arginine residue which was shown by site directed mutagenesis to play a key role in binding $NADP^+$, but not NAD^+ (*6*).

L. mesenteroides G6PD is a dimer of identical subunits of M_r 54 316 with 2 active sites per dimer, putatively located in a pocket between the coenzyme binding domain and the large $\beta+\alpha$ domain in each subunit (*5*). This pocket contains several amino acids that are completely conserved, including an eight-residue peptide (Figure 1). Since there is no requirement for a metal ion, one of these residues is likely to be the general base that abstracts a proton from the C1-hydroxyl group of G6P, allowing transfer of the C1-hydride to the nicotinamide ring of the coenzyme. On the basis of pH variation of kinetic parameters, Viola (*7*) proposed a carboxylate, probably from an aspartate or glutamate, as the catalytic base. However, chemical modification studies suggest that one or more histidine residues are important for catalytic activity of *L. mesenteroides* G6PD (*3*) and the G6PDs isolated from *Saccharomyces cerevisiae* (*8*) and *Candida utiliz* (*9*). From the X-ray structure of *L. mesenteroides* G6PD, the most likely candidate for the base is His-240, with its Nϵ2 optimally positioned for proton abstraction and its Nδ1 hydrogen bonded to the Oδ1 of Asp-177 (*5*). An equivalent catalytic dyad is found in several mechanistically unrelated enzymes, including 2-hydroxyacid dehydrogenases (*10*), phospholipase A2 (*11*), thermolysin (*12*), mandelate racemase (*13*), soluble epoxide hydrolase (*14*), various zinc containing enzymes (*15*), glutamate mutase (*16*), and as part of the catalytic triad of all the serine proteases (*17*). Although the location of His-178 makes it another candidate for the general base, it is bound to a phosphate ion (the precipitant for crystallization of the enzyme), and therefore is likely to be protonated. It was predicted that His-178 is an important residue in binding G6P (*5*).

In this investigation, we used site-directed mutagenesis to replace His-240, Asp-177, and His-178 with asparagine to assess their functions in the catalytic mechanism of G6PD. Decrease in catalytic activity in the mutant enzymes can result from several changes, including the removal of the general base (asparagine still has the capacity to form a hydrogen bond, but it cannot accept a proton from the C1 hydroxyl of G6P); removal of an amino acid that is essential

[†] Supported by Grant MCB-9513814 from the National Science Foundation.

[‡] The atomic coordinates of the H240N enzyme with NAD^+ (2dpg), and the H240N enzyme with $NADP^+$ (3dpg) have been deposited with the Brookhaven Protein Data Bank.

* Corresponding author. Phone: 315-443-3181. Fax: 315-443-2012; E-mail: hrlevy@mailbox.syr.edu.

[§] Syracuse University.

[||] University of Oxford.

[1] Abbreviations: G6PD, glucose 6-phosphate dehydrogenase; G6P, glucose 6-phosphate; PAGE, polyacrylamide gel electrophoresis; SDS, sodium dodecyl sulfate; S-NADPH, thionicotinamide-NADPH.

S0006-2960(97)02069-2 CCC: $15.00
Published on Web 02/12/1998

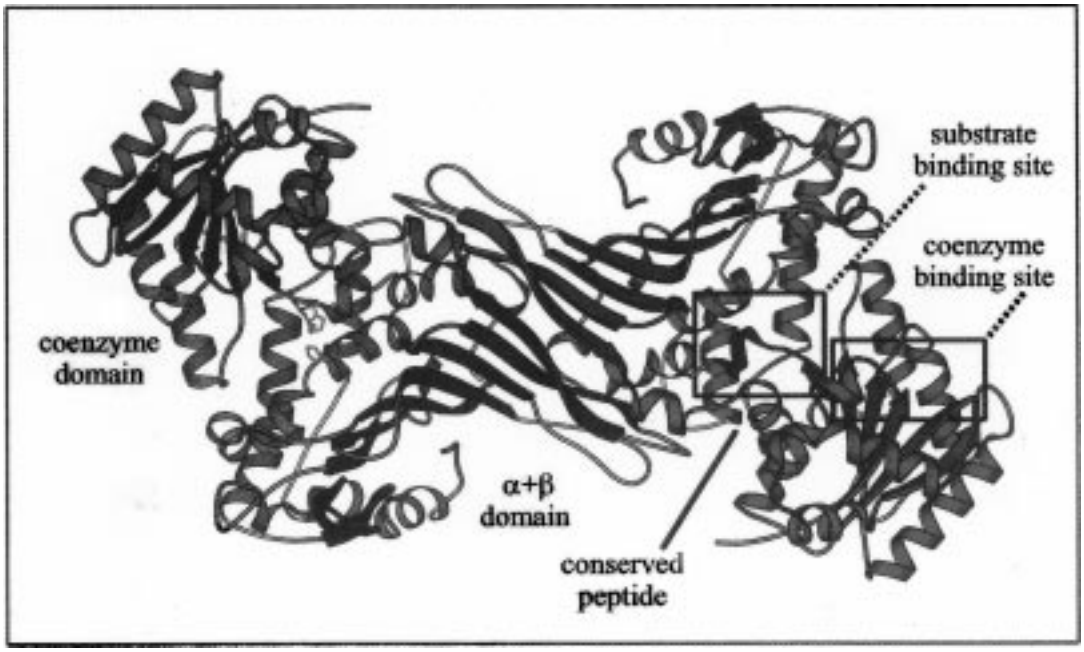

FIGURE 1: The *Leuconostoc mesenteroides* G6PD dimer viewed down the 2-fold axis. In the right-hand subunit, helixes are red, sheet strands green, and coils yellow. The substrate and coenzyme binding sites are indicated and the conserved peptide is colored blue. In the left-hand subunit, the domains are labeled and the residues Asp-177 (purple), His-178 (light blue), and His-240 (red) are drawn. The Figure is drawn, as are Figures 3 and 4, with a modified version of Molscript (*30*, *31*).

for binding substrate or coenzyme; and removal of an amino acid that is essential for maintaining the enzyme in a catalytically competent conformation. To distinguish among these possibilities, the mutated enzymes were characterized by substrate binding studies and steady-state kinetic analyses. The three-dimensional structure of H240N G6PD was determined at 2.5 Å resolution to characterize any structural alterations that might have resulted from this mutation.

The results suggest that His-240 is the general base that abstracts the proton from the C1-hydroxyl of G6P and that the carboxylate of Asp-177 stabilizes the positive charge that forms on His-240 in the transition state, forming a catalytic dyad. The results also confirm the postulated role for His-178 in binding the phosphate moiety of G6P.

EXPERIMENTAL PROCEDURES

Materials. NAD^+ and $NADP^+$ were obtained from Boehringer Mannheim; Matrex gel Purple A, Matrex gel Orange B, and CF-50 Centriflo membrane cones from Amicon Corp.; G6P and Protease X (thermolysin) from Sigma; D-glucose from Fisher; Coomassie protein assay reagent and bovine serum albumin standard from Pierce; Sequenase Version 2.0 DNA sequencing system and Sculptor in vitro mutagenesis system from Amersham International plc; Prep-A-Gene DNA purification system from Bio-Rad; pUC-19, M-13 bacteriophage, T4 polynucleotide kinase, and DNA ligase from Gibco-BRL; and restriction endonucleases from New England Biolabs. Oligonucleotides for site-directed mutagenesis were synthesized by Ransom Hill Bioscience Inc. The oligonucleotide sequences were as follows (changes from wild-type sequences are underlined): D177N, TTCCGTATTAACCACTAC; H178N, CGTATTGACAACTACCTTG; H240N, GATTCAAAACAACACCATGC.

Site-Directed Mutagenesis. All standard DNA techniques were performed as described by Sambrook et al. (*18*) and as previously described (*6*). Site-directed mutagenesis was performed with the Amersham in vitro mutagenesis system, using the oligonucleotides listed above. Mutations were constructed in M-13 bacteriophage, subcloned into pUC19, and transformed into *E. coli* strain SU294, which lacks the G6PD gene (*19*). Plasmids were isolated, and the entire G6PD gene was sequenced for each mutant to ensure that no other mutations were introduced.

Purification of G6PD and Assay of Activity. Recombinantly expressed native and mutant G6PDs were purified by the methods described previously (*19*) and judged to be homogeneous by SDS−PAGE of 5−10 μg of the enzymes with silver staining (data not shown). Routine assays for G6PD activity were performed at 25 °C in a Gilford 240 spectrophotometer at 340 nm by following the rate of appearance of NADPH. Assays were initiated by the addition of enzyme to 1.0 mL of 33 mM Tris-HCl, pH 7.6, containing 2.28 mM G6P and 0.160 mM $NADP^+$. Protein concentrations were routinely determined using the Coomassie reagent with bovine serum albumin as a standard (*20*). The concentration of wild-type enzyme was determined from its extinction coefficient at 280.5 nm (*21*), and from this a correction factor of 1.55 was calculated by which to multiply the values determined by the Bradford procedure. It was assumed that the extinction coefficients of the mutant G6PDs were the same as that of wild-type enzyme.

Determination of Kinetic Parameters. Kinetic measurements for the wild-type, D177N, and H178N enzymes were performed in duplicate or triplicate at 25 °C. Initial estimates of K_m values were determined by using one fixed substrate at a concentration of at least 20 times its wild-type K_m value and varying the concentration of the other substrate. Initial estimates were used to select appropriate concentrations for measuring the true K_m values. This was accomplished by preparing reaction mixtures containing five different concentrations of coenzyme, each at five different concentrations

Table 1: X-ray Data Collection Parameters and Statistics

data set, site, wavelength	resolution (Å)	R_{merge} overall (outer shell)	$I/\sigma I$ overall (outer shell)	completeness overall (outer shell)	redundancy	reflections measured	independent reflections	reflections > 2σ
type I, 9.5, 0.876 Å	2.5	8.0% (44.1%)	6.5 (2.4)	98.3% (97.6%)	2.1	48 970	23 319	19 472
type II, 9.5, 0.876 Å	2.5	10.4% (41.1%)	7.2 (1.9)	59.5% (56.1%)	1.7	23 907	14 062	10 054
type II, conventional source, 1.542 Å	3.5	17.0% (28.7%)	6.0 (3.1)	79.6% (69.6%)	2.8	20 930	7475	5546
type II, merged	2.5	8.0% (12.5%, 3.5 Å)	7.1 (2.2)	62.4%	1.3[a]	21 142	16 263	11 859

[a] Compared with the two separately merged data sets.

of G6P, and measuring the rate of appearance of reduced coenzyme at 340 nm after the addition of 10 μL of enzyme. Substrate and coenzyme concentrations ranged from 0.2 to 5 times their apparent K_m values. The concentrations of coenzyme and G6P solutions were determined enzymatically with G6PD. The quantities of the enzymes used in these determinations were 0.065 μg of wild-type, 0.8 μg of H178N, and 6.3 μg of D177N. The pH of reaction mixtures was measured after the reaction, and never deviated more than $\pm$0.2 pH units from the pH of the buffer. The data were analyzed using the SEQUEN program for true kinetic constants and the HYPER program for apparent kinetic constants (*22*).

For H240N G6PD, apparent kinetic constants were determined in assays using 50 μg of enzyme over a 30 min period in a Gilford Response spectrophotometer. Controls either contained no enzyme or no G6P. The activity was directly proportional to the enzyme concentration.

Determination of Substrate Binding Constants. Binding constants for G6P and D-glucose were determined for the wild-type enzyme by the method described previously (*23*). Appropriate concentrations of the mutant enzymes (1.0 mg/mL H240N, 0.5 mg/mL of D177N, or 0.05 mg/mL of H178N) were incubated with thermolysin and various concentrations of G6P or D-glucose at 40 °C. At various time intervals, aliquots were removed, diluted in ice-cold H_2O, and assayed in duplicate or triplicate. Data were analyzed as previously described (*23*), except that percent protection versus substrate concentration curves were analyzed using a nonlinear regression fit (Ultrafit).

Crystallization and Structure Determination of H240N G6PD. Crystals of H240N G6PD were grown from unbuffered ammonium sulfate. Before crystallization, the protein was dialyzed extensively in 0.1 M Tris-HCl, pH 7.5. Crystals were grown in the presence of either G6P and NAD^+ (type I) or G6P and $NADP^+$ (type II). The hanging drop vapor diffusion method was used with the well containing 2.27 M ammonium sulfate (unbuffered). The drops contained 4.8 mg/mL H240N G6PD in Tris-HCl and were 25 mM in G6P. Either NAD^+ to a concentration of 12.5 mM or $NADP^+$ to 0.500 mM concentration was added; coenzyme solution was buffered to pH 5.8. Initially, an equal volume of well buffer was added to the drop. The crystals used in the analysis grew to $(1.5 \times 0.1 \times 0.1)mm^3$.

The crystals grow in spacegroup $P6_222$, with cell dimensions $a = b = 137.0$ Å, $c = 121.2$ Å, $\alpha = \beta = 90°$, $\gamma = 120°$ (Type I); or $a = b = 136.9$ Å, $c = 121.3$ Å $\alpha = \beta = 90°$, $\gamma = 120°$ (Type II). Both types are isomorphous with crystals of an $NADP^+$ complex of the cysteine mutant Q365C G6PD (*24*) grown from ammonium sulfate under similar conditions (manuscript in preparation).

Data were collected to 2.5 Å resolution at the CCLRC Daresbury Laboratory synchrotron on beamline 9.5, at wavelength (λ) 0.876 Å. All intensity data were recorded on a Mar Research image plate. For crystal type I, the data were 97% complete; for type II, a 60% complete data set was obtained; this was supplemented by data collected to 3.5 Å on a conventional source $\lambda = 1.5418$ Å. All data sets were processed using the program suite Denzo (*25*) followed by programs in the CCP4 package (*26*). Data collection parameters and statistics are given in Table 1.

Rigid body refinement was carried out using the program X-PLOR (*27*) and the refined model of the isomorphous protein Q365C G6PD, without solvent or coenzyme. Randomly chosen test sets (5% of the data) were selected for each crystal type for independent monitoring of the refinement (R_{free}).

Difference maps were calculated using the rigid-body refined model; these showed that neither G6P nor NAD^+ had bound in crystal type I, while there was evidence of a low occupancy of $NADP^+$ but no G6P in crystal type II. Both data sets were taken through cycles of model building, which included addition of a fragment of $NADP^+$ to crystal type II, adding well-bound waters, and further refinement. Final statistics after refinement are given in Table 2. Since the overall conformation of the protein in type I and type II crystals differed little from that of the isomorphous $NADP^+$ bound Q365C G6PD structure (the rms deviation for all main-chain atoms being 0.27 Å for data set I and 0.26 Å for data set II), for the less complete data set, Type II, the side-chain conformation of the high-resolution Q365C G6PD was accepted unless difference maps showed that movement was required.

RESULTS AND DISCUSSION

G6PD Isolation and Activity. While the mutant enzyme D177N could be detected in the same way as the wild-type enzyme, the mutant enzymes H178N G6PD and H240N G6PD lacked sufficient activity for detection in our standard assay system. Increasing the G6P concentration to 22.8 mM was sufficient to detect activity with the H178N enzyme and to monitor purification of this enzyme. Fractions containing the H240N enzyme were located by SDS−PAGE with silver staining, and the presence of purified H240N G6PD was confirmed by western blotting with a monoclonal antibody prepared against native *L. mesenteroides* G6PD (*28*).

Purified H240N G6PD was concentrated 6-fold on a CF-50 Centriflo membrane cone and tested for activity in our standard assay system. Preliminary experiments showed that H240N activity is detectable and proportional to enzyme concentration, and follows Michaelis−Menten kinetics (data

Table 2: Refinement Statistics

data set	type I, H240N crystallized in the presence of NAD^+ and G6P	type II, H240N crystallized in the presence of $NADP^+$ and G6P
reflections included (25−2.5 Å resolution)[a]	22 111 (1122)[b]	15 455 (1211)
R, (R_{free})[c] initial (%)	29.4 (31.2)	27.9 (28.1)
R, (R_{free}) after rigid body refinement of protein only (%)	22.0 (24.3)	21.2 (25.0)
R, (R_{free}) final (%)	16.8 (21.4)	17.3 (23.2)
parameters refined	15960	15772
percent residues in most favored region Ramachandran plot[d]	90.9	87.4
mean temperature factor (main chain, side chain)	30.6 (33.1)	29.7 (31.9)
waters included	137	73
mean temperature factor of waters	32.0	30.0

[a] A bulk solvent contribution was modeled for both data sets (set A: $k = 0.35$e Å^{-3}, $B = 45$ Å^2, set B: $k = 0.41$e Å^{-3}, $B = 65$ Å^2) enabling data between 25 and 8 Å resolution to be included in the refinement. [b] Number in parentheses is number of test reflections not used for refinement but used to calculate R_{free}. [c] An independent test set of reflections was chosen for each data set. It is now clear that this procedure might lead to a low value of R_{free} since the test reflections had been included in the refinement of an isomorphous data set; a more satisfactory procedure would have been to choose the same reflections as had been used in the initial $P6_222$ structure. [d] Supplied in Supporting Information.

Table 3: Kinetic Data for NADP-Linked Reaction for Wild-Type and Mutant G6PDs[a]

enzyme	$K_{m,G6P}$ (μM)	$K_{m,NADP^+}$ (μM)	$K_{i,NADP^+}$ (μM)[c]	k_{cat} (min^{-1})[d]	$k_{cat}/K_{m,G6P}$ (min^{-1}, μM^{-1})[d]	$k_{cat}/K_{m,NADP^+}$ (min^{-1}, μM^{-1})[d]
wild-type[b]	114 ± 11	8.0 ± 0.7	3.4 ± 1	20 200	178	2530
D177N	117 ± 15	8.2 ± 0.8	15.0 ± 4	66	0.56	7.8
H178N	42 900 ± 6 400	15.2 ± 2.0	3.7 ± 2	833	0.02	55
H240N[e]	1280 ± 120	8.8 ± 0.9		0.40	0.0003	0.05

[a] Kinetic constants ±SE. [b] Data from Lee and Levy (*19*). The k_{cat} value has been adjusted to reflect the correct protein concentration determined from the extinction coefficient (see Experimental Procedures). [c] K_i calculated from kinetic mechanism which for the NADP-linked reaction is ordered sequential with $NADP^+$ binding first (*2*). [d] Per mole of enzyme subunit. [e] Apparent values.

Table 4: Kinetic Data for NAD-Linked Reaction for Wild-Type and Mutant G6PDs[a]

enzyme	$K_{m,G6P}$ (μM)	K_{m,NAD^+} (μM)	k_{cat} (min^{-1})[d]	$k_{cat}/K_{m,G6P}$ (min^{-1}, μM^{-1})[c]	$k_{cat}/K_{m,NAD^+}$ (min^{-1}, μM^{-1})[c]
wild-type[b]	69 ± 9.0	160 ± 18	43 600	630	269
D177N	290 ± 35	1 430 ± 330	291	1.0	0.2
H178N	13 600 ± 2 600	950 ± 200	2850	0.2	3.0
H240N[d]	800 ± 160	810 ± 20	1.2	0.001	0.001

[a] Kinetic constants ±SE. (K_i cannot be calculated from steady-state random kinetic mechanism). [b] Data from Lee and Levy (*19*). The k_{cat} value has been adjusted to reflect the correct protein concentration determined from the extinction coefficient (see Experimental Procedures). [c] Per mole of enzyme subunit. [d] Apparent values.

not shown). This concentrated enzyme was used to determine apparent kinetic constants described below.

Preliminary NADP-linked assays with purified H178N G6PD showed a pattern of substrate inhibition at high concentrations of G6P and low concentrations of $NADP^+$, which was overcome with progressively higher concentrations of $NADP^+$ (data not shown). For the NAD-linked reaction, no inhibition was observed. These results are consistent with the difference in the kinetic mechanisms for the NADP- and NAD-linked reactions (*2*). Since the NADP-linked reaction is ordered sequential with $NADP^+$ binding first, at high G6P concentrations (20 times K_d), the predominant enzyme form is the enzyme−G6P binary complex, which cannot bind $NADP^+$ productively. Therefore, to determine kinetic constants for the NADP-linked reaction for H178N G6PD, assays were carried out with G6P concentrations that did not produce inhibition.

Effects of Amino Acid Substitutions on Kinetic Constants. The most striking result is the dramatic reduction in catalytic activity when His-240 is replaced with Asn, which is due predominately to a decrease in k_{cat} (Tables 3 and 4). The H240N enzyme has a (4×10^4)-fold and (5×10^4)-fold reduction in k_{cat} for the NAD- and NADP-linked reactions, respectively. The K_m value for $NADP^+$ is similar to that of wild-type G6PD, while the K_m for NAD^+ increases 5-fold. The K_m for G6P is increased by an order of magnitude in both reactions.

When Asp-177 is replaced with Asn, the k_{cat} decreases by more than 2 orders of magnitude in both reactions (Tables 3 and 4). The K_m values for G6P and coenzyme in the NADP-linked reaction are similar to those of wild-type G6PD; however, in the NAD-linked reaction they increased 4-fold and 9-fold, respectively.

As predicted from the inorganic phosphate binding site in the apo-enzyme (*5*), substitution of His-178 with Asn results in a dramatic increase in the K_m value for G6P: 200-fold and 400-fold increases were seen in the K_m for G6P in the NAD- and NADP-linked reactions, respectively (Tables 3 and 4). While the K_m and K_i values for $NADP^+$ are similar to those for wild-type G6PD, the K_m for NAD^+ increases 6-fold. The second-order rate constant (k_{cat}/K_m) for G6P decreases by (3×10^3)-fold and (9×10^3)-fold in the NAD- and NADP-linked reactions, respectively, whereas the k_{cat}/K_m for either coenzyme decreases only (*50−90*)-fold. These results suggest that replacing His-178 with Asn primarily affects the enzyme's interaction with substrate. There is also

a smaller but significant effect on k_{cat}, which decreases by approximately an order of magnitude in both reactions.

These results are consistent with the hypothesis that His-240 is the general base that abstracts the C1−OH proton from G6P, and that His-178 is an important residue in binding G6P. Changing Asp-177 to Asn causes a significant decline in k_{cat}, suggesting that Asp-177 is involved in catalysis. However, in the crystal structure of the apo-enzyme, crystallized from phosphate, the Oδ1 atom of Asp-177 is H-bonded to the Nδ1 of His-240 (*5*); thus, it is likely that Asp-177 functions to make His-240 a better general base. This hypothesis is currently under investigation.

Contribution of His-178 in the Transition State. The change in the free energy of activation for the reaction of the mutant enzyme relative to wild-type enzyme, ΔG_Y, where the amino acid that undergoes mutation is not involved in the chemical steps of the reaction, can have contributions from several sources. These include changes in the free energy of substrate binding in the transition state as well as free energy changes involved in varying substrate orientation and changes in the detailed conformation of the active-site residues. This value may be calculated from the equation

$$\Delta G_Y = RT \ln\left[\frac{(k_{cat}/K_m)_{mut}}{(k_{cat}/K_m)_{wt}}\right] \quad (1)$$

where Y = the amino acid side chain in the wild-type (wt) enzyme, and mut refers to mutant enzyme (*29*). For H178N G6PD this value is approximately 4.7 and 5.4 kcal/mol, in the NAD- and NADP-linked reactions, respectively. If it can be assumed that the side chain of Asn-178 in H178N G6PD does not interact with G6P and that the mutation does not otherwise change the G6P site, ΔG_Y could be attributed to the contribution of His-178 to the binding free energy of G6P in the transition state.

Substrate Binding Studies. Since the H240N enzyme has small but detectable catalytic activity, thermodynamic dissociation constants were determined by measuring protection from proteolytic degradation by various concentrations of G6P. This method has been used before to determine G6P K_d values for the wild-type enzyme that are in reasonably good agreement with values derived using other methods (*23*). Various concentrations of G6P were incubated with either wild-type or mutant G6PDs in the presence of thermolysin at 40 °C, and at various time intervals, aliquots were removed, diluted into ice-cold H_2O, and assayed for activity under standard assay conditions. Figure 2a shows a semilog plot of percent remaining activity versus time for the H240N mutant enzyme with increasing concentrations of G6P. Since the semilog plots were in all cases linear, the derived first-order rate constants were used to calculate percent protection as previously described (*23*). Figure 2b shows the dependence of percent protection on G6P concentration for the H240N enzyme. As with all *L. mesenteroides* G6PDs assayed in this manner, G6P protected the enzyme in a saturable manner, allowing the calculation of K_d values using a nonlinear regression fit.

As expected, the largest change in the G6P K_d value results from substituting His-178 with Asn; K_d increases by an order of magnitude relative to that for wild-type G6PD (Table 5). When His-240 is replaced by Asn, the G6P K_d increases 4-fold, whereas the G6P K_d decreases 2-fold when Asp-177 is replaced with Asn. These results are consistent with the steady-state kinetic analyses, and suggest that His-178 is an important residue for G6P binding. The standard free energy of binding G6P to wild-type G6PD in the binary complex, calculated from the K_d is approximately 4.0 kcal/mol (Table 5). When His-178 is replaced with Asn, this value drops to 2.6 kcal/mol, indicating that the side chain of His-178 contributes ~1.4 kcal/mol *net* to binding G6P in the binary complex.

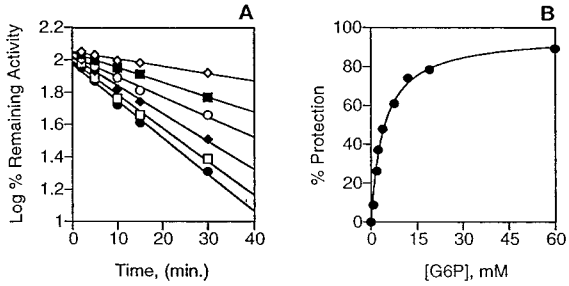

FIGURE 2: Determination of dissociation constants for G6P for wild-type and mutant G6PDs. Dissociation constants were determined by measuring protection from proteolytic degradation by various concentrations of G6P. (A) Representative semilog plot of percent remaining activity versus time (min) for the H240N enzyme. The concentrations of G6P were (●) 0 mM; (□) 0.8 mM; (◆) 2 mM; (○) 4 mM; (■) 8 mM; (◇) 19 mM. The derived first order rate constants were used to calculate percent protection by the method described previously (*24*). (B) Representative plot of percent protection versus G6P concentration for H240N G6PD. Dissociation constants were obtained from a nonlinear least-squares regression fit to an equation for ligand binding with one binding site (Ultrafit).

Table 5: Substrate Binding Constants for Wild-Type and Mutant G6PDs

enzyme	$K_{d,G6P}$[a] (mM)	$K_{d,Glucose}$[a] (mM)	$\frac{K_{d,Glucose}}{K_{d,G6P}}$	$\Delta G°_{G6P}$ (kcal/mol)
wild-type	1.2 ± 0.1[b]	952 ± 36	793	4.0
H178N	12.5 ± 2.1	404 ± 55	32	2.6
H240N	4.9 ± 1.0	855 ± 190	174	3.1
D177N	0.7 ± 0.2	372 ± 79	531	4.3

[a] K_d values ±SE were calculated by nonlinear least−squares fitting of the data to an equation for ligand binding with one binding site (Ultrafit). [b] From Kurlandsky et al. (*23*).

To determine if His-178 is a ligand to the phosphate moiety of G6P, we measured the K_d for D-glucose in the same manner as for G6P (Table 5).[2] Substituting His-178 with Asn results in a 2-fold decrease in the K_d for D-glucose relative to that for wild-type G6PD. However, the H178N enzyme has a decreased ability to discriminate effectively between D-glucose and G6P; the ratio between the K_ds for D-glucose and G6P is significantly diminished compared to wild-type G6PD (Table 5). This result suggests that His-178 is an important ligand to the phosphate moiety of G6P, which presumably interacts through a hydrogen bond and a charge−charge interaction. This confirms the original hypothesis concerning the binding of inorganic phosphate to crystals of the apo-enzyme (*5*), which would be better described as an enzyme−phosphate inhibitor complex. This

[2] Viola (*7*) showed that glucose is a substrate for *L. mesenteroides* G6PD in the presence of phosphate and/or dimethyl sulfoxide. We have found that glucose is utilized by the wild-type enzyme and D177N and H178N mutant enzymes in the absence of phosphate or dimethyl sulfoxide.

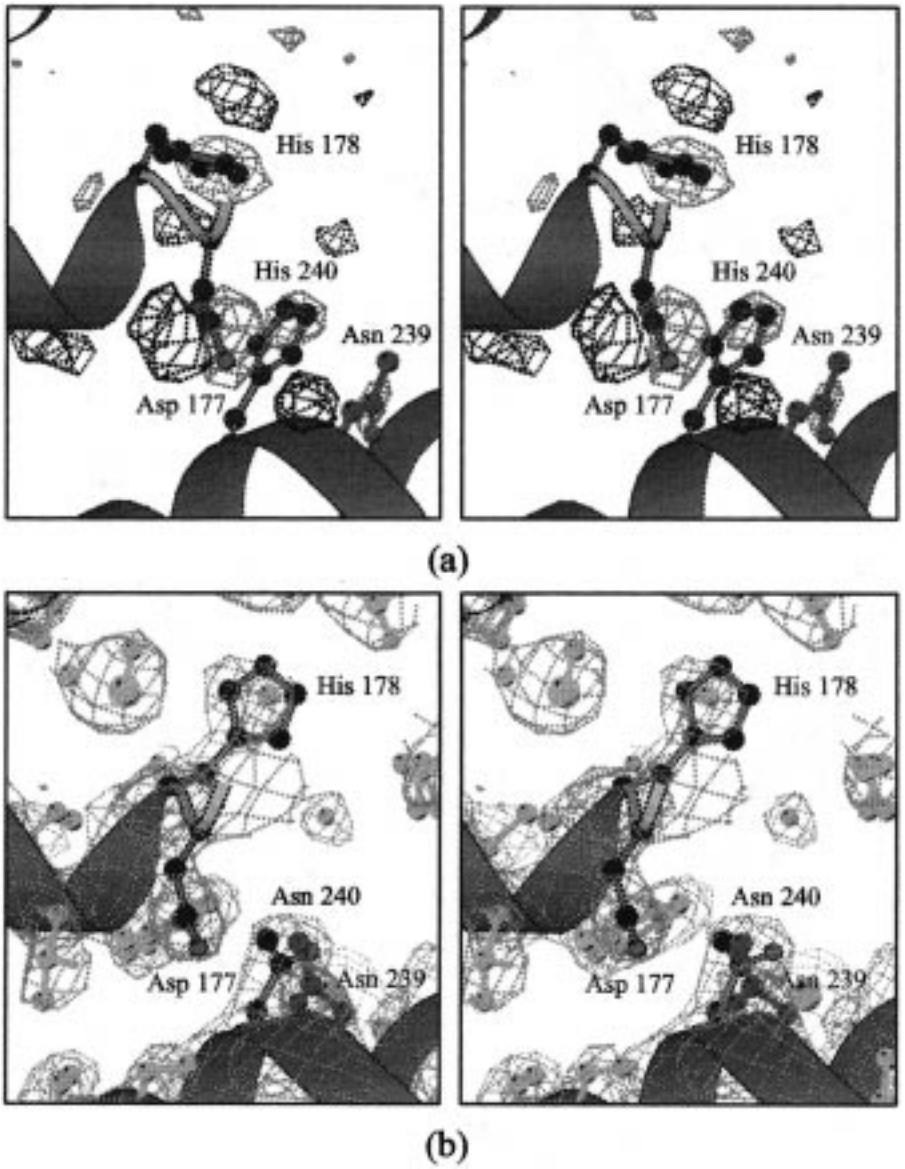

FIGURE 3: (a) Original difference electron density map for H240N mutant G6PD contoured at 3σ (stereoview), positive difference density blue, negative red. The model is the Q365C−$NADP^+$ complex. Replacing His-240 with Asn causes movement of Asp-177, His-178, and Asn-239. (b) Final ($2F_o - F_c$) map for H240N (type I) contoured at 1.25σ (stereoview), with final coordinates for this mutant. (Asn-240, Asp-177, and His-178 are in atom color, Asn-239 in dark gray, unperturbed coordinates in pale gray).

structure shows His-178 bound to two inorganic phosphate ions in one subunit and one in the other.

Substitution of Asp-177 with Asn results in small changes in the relative abilities to bind G6P and D-glucose (Table 5). The K_d for G6P decreases less than 2-fold in the D177N enzyme. While the K_d for glucose decreases almost 3-fold, the ratio between the K_ds for D-glucose and G6P is similar to that for wild-type G6PD. These results suggest that changing Asp-177 to Asn has little effect on the enzyme's ability to discriminate between G6P and D-glucose.

Substitution of His-240 with Asn results in a 4-fold increase in the K_d for G6P (Table 5). One explanation for this change is that the interaction of Nϵ2 of His-240 and the C1−OH of G6P contributes to the binding energy. The movement of other G6P binding residues through changes in the hydrogen-bonding network could also account for this difference. To distinguish between these possibilities, we determined the K_d for D-glucose in the H240N enzyme since the direct contribution of the His-240 Nϵ2 could be expected to affect the affinity for glucose by an equivalent amount if it bound in an identical manner. However, as demonstrated in Table 5, the K_d value for D-glucose is similar to that for wild-type G6PD, suggesting that the increase in the K_d for G6P in the H240N enzyme is due to a decrease in the affinity for the phosphate moiety of G6P, presumably due to the movement of other G6P binding residues.

The Three-Dimensional Structure of H240N G6PD. To assess the structural implications of mutating His-240 in the catalytic mechanism of G6PD, the H240N enzyme was crystallized and the three-dimensional structure was solved to a resolution of 2.5 Å by X-ray crystallography. The G6PD dimer is shown, annotated, in Figure 1. The major difference between the structure of the $NADP^+$ binary complex and that of each of types I and II of the H240N mutant corresponds to substitution of His 240 with the smaller Asn and a linked movement of Asp-177 and His-178. The initial difference electron density map is shown in Figure 3a with the Q365C $NADP^+$ structure in this region superimposed.

Figure 3b shows the final $2F_o - F_c$ map for the same region of the type I crystal with the refined H240N coordinates. The average difference in the main chain coordinates between the Q365C $NADP^+$ binary complex and each of the two structures discussed here (types I and II, see Experimental Procedures) was less than 0.3 Å for all main-chain coordinates. There were no changes at the secondary structure level, and the mean difference for side chain atoms was 0.37 Å for the 1887 equivalent atoms. NAD^+ did not bind to crystals (type I) of the H240N mutant in these conditions (neither has it been possible to bind NAD^+ to the Q365C mutant in this crystal form). In the H240N $NADP^+$ complex (type II), the coenzyme site was only partially occupied; the nicotinamide nucleotide was not ordered in this complex. G6P was not bound in either complex; it has subsequently been found that G6P does not bind to the Q365C mutant of G6PD under these crystallization conditions; the lack of G6P binding to the H240N mutant is to be expected considering its lower affinity in this mutant as determined by the binding study above. There are 36 residues (279 atoms) within 10 Å of the α carbon of His-240 (or Asn-240). The mean positional difference between the Q365C structure and either H240N structure for all atoms of these residues was 0.39 Å. Coordinates from the two crystals (types I and II) are essentially identical in this region and further discussion will be based on the binding site of H240N G6PD grown in the presence of NAD^+ and G6P (type I).

The active-site region is seen in Figure 4; the structure of the H240N mutant is superimposed on that of the Q365C mutant in Figure 4c. Of the main chain of Asn-240, the peptide nitrogen and Cα atoms do not move with respect to the equivalent atoms in His-240. The carbonyl oxygen moves 0.7 Å, the side chain amide group is within 0.4 Å of the corresponding Cγ, Cδ2, and Nδ1 of His-240. The side chain of Asp-177, however, has moved 1.4 Å away from Oδ1(Nδ2) of Asn-240; there is no hydrogen bond between Asp-177 Oδ1 and the Asn side chain, while there is a good hydrogen bond (2.7 Å) between His-240 Nδ1 and Asp-177 Oδ1. In the apo-enzyme and in the Q365C $NADP^+$ binary complex, a second hydrogen bond to Asp-177 is made to a water; also Asn-239 Nδ2 interacts with the carbonyl oxygen of Asp-235. In the H240N crystal, the Asn-239 side chain prefers to interact directly with Asp-177 Oδ2. The main chain of Asp-177 moves in the H240N crystal (Cα of Asp-177 moves 1.4 Å), accommodating the longer distance from residue 240, as does the main chain of His-178. Presumably, as a result of the loss of the Asp-177/His-240 hydrogen bond, and the consequent movement of the peptide, the side chain of His-178 rotates so that Nδ1 moves 2 Å and Nε2 moves 4 Å. The different hydrogen bond networks in the region of His-240 (in the Q365C G6PD−NADP complex) and in the same area close to Asn-240 of H240N G6PD can be compared in Figure 4, panels a and b.

In the Q365C G6PD−$NADP^+$ complex in this space group, a sulfate ion may be seen bound to Nε2 of His-178, in a position corresponding to the outer phosphate ion in subunit A of the apo-enzyme. The ligands to both the outer phosphate and to the sulfate are His-178 Nε2, Tyr-179 Oη, Lys-182 Nζ, and Lys-343 Nζ. This sulfate ion is absent from both types of H240N crystals. The movement of His-178 resulting from the H240N mutation distorts any putative G6P phosphate site in this region. The different oxygens of an enzyme-bound phosphate or sulfate may have hydrogen bonds to different protein ligands. In subunit A of the apo-enzyme (*5*) and in the $NADP^+$ complex isomorphous with the H240N mutant, His-178, Tyr-179, and Lys-182 form a triangular template for the phosphate or sulfate. The distances between His-178 Nε2 and Tyr-179 Oη and His-178 Nε2 and Lys-182 Nζ are close to 5 Å. Distances between the different H-bond donor ligands to the phosphate should be no longer than 7.5 Å to give hydrogen bonds which are reasonably linear. However, in the H240N structure, His-178 Nε2 is more than 9 Å from the remaining ligands to the phosphate and the triangular arrangement of ligands is lost. The residues involved in binding to the sulfate ion and assumed to bind to the G6P phosphate are also seen in Figure 4, panels a and b.

Since the glucose binding experiments discussed above show that His-178 is important for binding the phosphate moiety of G6P, the movement of His-178 in the H240N enzyme most likely accounts for the increase in the K_m and K_d values for G6P and is consistent with the conclusions from the H240N glucose binding experiment. It is not likely that this movement accounts for the large decline in k_{cat} in the H240N enzyme since replacement of His-178 with Asn results in an enzyme that is only an order of magnitude less active than wild-type G6PD, making it unlikely that His-178 is the general base.

The Catalytic Mechanism of G6PD. The oxidation of glucose 6-phosphate by G6PD involves general base abstraction of a proton from the C1−OH, thereby allowing transfer of the hydride from C1 to the C4 position of the nicotinamide ring of the coenzyme. The X-ray crystal structure and the changes in catalytic and binding constants resulting from site-directed mutagenesis described here suggest that the imidazole side chain of His-240 is the general base. When His-240 was replaced with Asn, the apparent k_{cat} decreased by approximately 10^4-10^5-fold in both the NAD- and NADP-linked reactions (Tables 3 and 4), with only a small decrease in the enzyme's ability to bind G6P (Table 5), which is attributed to movement of His-178 (Figure 4, panels b and c).

Viola (*7*) proposed, on the basis of the dependence of k_{cat} and k_{cat}/K_m on pH for the NADP-linked reaction, that the catalytic base was likely to be an aspartate or glutamate. The only amino acid with a carboxyl group that is conserved and in a position in the three-dimensional structure to be a candidate for the general base is Asp-177 (*5*). When Asp-177 was replaced with Asn, the k_{cat} decreased 2 orders of magnitude with only small changes in the other kinetic parameters (Tables 3 and 4). However, it can also be seen from the apo-enzyme structure (*5*) that the Asp-177 carboxyl would not be accessible to G6P bound to His-178. These results suggest that Asp-177 is involved in catalysis, but not as the general base that abstracts the proton from the C1−OH of G6P. The decrease in k_{cat} by 4 orders of magnitude in the H240N complex leads to our proposal that His-240 fulfills this role, and that Asp-177 is hydrogen bonded to it and participates in catalysis by stabilizing the positive charge that forms on His-240 in the transition state, forming a catalytic dyad (Scheme 1). This was originally suggested on the basis of the crystal structure of the apo-enzyme crystallized from phosphate (*5*).

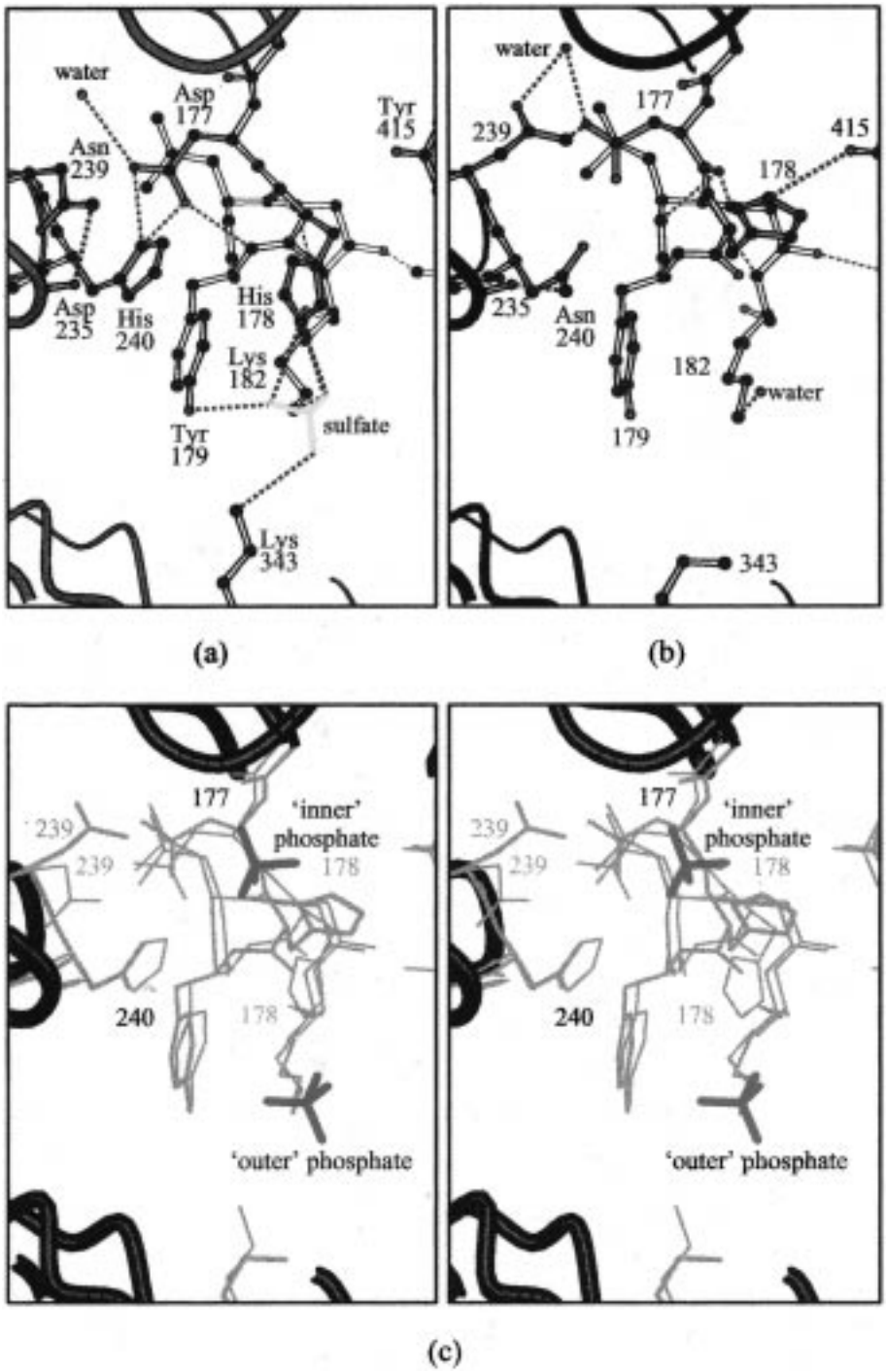

FIGURE 4: Active-site region. (a) Hydrogen bonding in Q365C G6PD, crystallized isomorphously with the H240N mutant from ammonium sulfate. His-240 Nδ1 interacts with Asp-177 Oδ1 (and Oδ2); Asp-177 Oδ1 also H-bonds Tyr-179 −NH and Oδ2 a water. Asn-239 Nδ2 interacts with the carbonyl of Asp-235. His-178 Nϵ2, Tyr-179 Oη, Lys-182 Nζ, and Lys-343 Nζ are ligands to the sulfate ion (yellow). Residues 177, 178, 239, and 240 are in cyan. (b) Hydrogen bonding in H240N G6PD. Asn-240 Nδ2 interacts with the carbonyl oxygen of Asp-235. There is *no* hydrogen bond between Asn-240 and Asp-177; instead Asp-177 Oδ2 interacts with Asn-239 Nδ2. The rotated His-178 Nϵ2 hydrogen bonds the carbonyl of Tyr-415. Since His-178 has moved, there is no binding site for a sulfate ion. Residues 177, 178, 239, and 240 are in pink. (c) Superposition (stereoview) of active site residues of H240N G6PD (pink) and Q365C G6PD (cyan), orientation as in panel a and b. The rotation of the His-178 side chain is apparent. The two phosphate ions bound in subunit A of the apo-enzyme are superimposed (red); the outer phosphate takes up the same position as the sulfate in panel a.

CONCLUSIONS

In this paper, evidence is presented that His-240 is the general base that abstracts a proton from the C1−OH of G6P in the mechanism catalyzed by glucose-6-phosphate dehydrogenase from *L. mesenteroides*. A model for the mechanism is proposed that includes a role for Asp-177 in stabilizing the positive charge that forms on His-240 in the transition state, forming a catalytic dyad. His-178 is shown to be an important residue that participates in binding the phosphate moiety of G6P. Since all the amino acid residues discussed in this paper are conserved in the 27 G6PDs that have been sequenced to date (M. J. Adams, unpublished alignment), it is likely that the mechanism proposed here can be generalized for all G6PDs. G6PD is another example

Scheme 1. Proposed Catalytic Mechanism for the Reaction Catalyzed by G6PD[a]

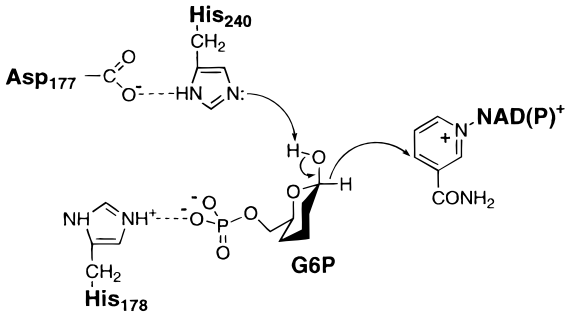

[a] The Nδ1 atom of His-240 is hydrogen bonded to the Oδ1 atom of Asp-177, forming a catalytic dyad. The Nε2 of His-240 is poised to act as a general base by abstracting a proton from the C1−OH of G6P, allowing transfer of the C1-hydride to the C4 position of the nicotinamide ring of $NAD(P)^+$.

of the growing list of proteins that have been shown to utilize the His/Asp catalytic dyad for a variety of catalytic and structural functions.

ACKNOWLEDGMENT

We gratefully acknowledge technical assistance from Valarie E. Vought and Xiaohong Yin. We thank the Wellcome Trust for a Wellcome Prize Studentship to CEN (1993−97); Dr. S. Gover for helpful discussion and for drawing the final versions of Figures 1, 3, and 4; Dr. A. K. Basak for helpful discussion; the support staff, station 9.5 at CCLRC Daresbury Laboratory, Warrington, U.K.; and Prof. Louise N. Johnson for facilities and support. Monoclonal antibody was generously supplied by Dr. Mark Levy of Syva Company, Palo Alto, CA. M.J.A. is the Dorothy Hodgkin−E.P. Abraham Fellow of Somerville College, Oxford, and an associate member of the Oxford Centre for Molecular Sciences.

SUPPORTING INFORMATION AVAILABLE

Ramachandran plots for H240N *L. mesenteroides* G6PD types I and II are available (2 pages). Ordering information is given on any current masthead page.

REFERENCES

1. Levy, H. R. (1989) *Biochem. Soc. Trans. 17*, 313−315.
2. Levy, H. R., Christoff, M., Ingulli, J., and Ho, E. M. L. (1983) *Arch. Biochem. Biophys. 222*, 473−488.
3. Haghighi, B. and Levy, H. R. (1982) *Biochemistry 21*, 6429−6434.
4. Lee, W. T., Flynn, T. G., Lyons, C., and Levy, H. R. (1991) *J. Biol. Chem. 266*, 13028−13034.
5. Rowland, P., Basak, A. J., Gover, S., Levy, H. R., and Adams, M. J. (1994) *Structure 2*, 1073−1087.
6. Levy, H. R., Vought, V. E., Yin, X., and Adams, M. J. (1996) *Arch. Biochem. Biophys. 326*, 145−151.
7. Viola, R. E. (1984) *Arch. Biochem. Biophys. 228*, 415−424.
8. Kim, Y. S., Yong, I. K., and Byun, H. S. (1988) *Biochem. Int. 17*, 1099−1106.
9. Domschke, W., Engel, H. J., and Domagk, G. F. (1969) *Hoppe-Seyler Z. Physiol. Chem. 351*, 1117.
10. Birktoft, J. J., and Banaszak, L. J. (1983) *J. Biol. Chem. 258*, 472−482.
11. Dijkstra, B. W., Drenth, J., Kalk, K. H., and Hartley, B. S. (1981) *Nature 289*, 604−606.
12. Weaver, L. H., Kester, W. R., and Mathews, B. W. (1977) *J. Mol. Biol. 114*, 119−132.
13. Neidhart, D. J., Howell, P. L., Petsko, G. A., Powers, V. M., Li, R., Kenyon, G. L., and Gerlt, J. A. (1991) *Biochemistry 30*, 9264−9273.
14. Pinot, F., Grant, D. F., Beetham, J. K., Parker, A. G., Borhan, B., Landt, S., Jones, A. D., and Hammock, B. D. (1995) *J. Biol. Chem. 270*, 7968−7974.
15. Christianson, D. W., and Alexander, R. S. (1989) *J. Am. Chem. Soc. 111*, 6412−6419.
16. Chen, H.-P., and Marsh, E. N. G. (1997) *Biochemistry 36*, 7884−7889.
17. Kraut, J. (1977) *Annu. Rev. Biochem. 46*, 331−358.
18. Sambrook, J., Fritsch, E. F., and Maniatis, T. (1989) *Molecular Cloning: A Laboratory Manual*, 2nd ed., Cold Spring Harbor Laboratory Press, Plainview, NY.
19. Lee, W. T., and Levy, H. R. (1992) *Protein Sci. 1*, 329−334.
20. Bradford, M. (1976) *Anal. Biochem. 72*, 248−254.
21. Olive, C., and Levy, H. R. (1971) *J. Biol. Chem. 246*, 2043−2046.
22. Cleland, W. W. (1979) *Methods Enzymol. 63*, 103−135.
23. Kurlandsky, S. B., Hilburger, A. C., and Levy, H. R. (1988) *Arch. Biochem. Biophys. 264*, 93−102.
24. Adams, M. J., Basak, A. K., Gover, S., Rowland, P., and Levy H. R. (1993) *Protein Sci. 2*, 859−862.
25. Otwinowski, Z. (1993) Oscillation Data Reduction Program. *Data Collection and Processing. Proceedings of the CCP4 Study Weekend*, pp 56−62, SERC, Daresbury Laboratory, Warrington, U.K.
26. Collaborative Computational Project, No. 4 (1994) *Acta Crystallogr. D50*, 760−763.
27. Brunger, A. T. (1992) *X-plor. Version 3.1. A System for X-ray Crystallography and NMR*, New Haven and London, Yale University Press.
28. Skold, C., Gibbons, I., Gould, D., and Ullman, E. D. (1987) *J. Immunol. 138*, 3408−3414.
29. Wilkinson, A. J., Fersht, A. R., Blow, D. M., and Winter, G. (1983) *Biochemistry 22*, 3581−3586.
30. Kraulis, P. J. (1991) *J. Appl. Crystallogr. 24*, 946−950.
31. Esnouf, R. M. (1997) *J. Mol. Graphics 15*, 132−134.

BI972069Y